In:
Stratified Flows:
Proceedings of the Third International Conference
On Stratified Flows, February 3-5, 1987
Pasadena, CA
E.J. List and G.H. Jirka (eds.)
American Society of Civil Engineers
New York
1990

VARIABILITY OF PHYSICAL, CHEMICAL, AND BIOLOGICAL PARAMETERS IN THE VICINITY OF AN OCEAN OUTFALL PLUME

B. H. Jones[1], A. Bratkovich[1], T. Dickey[1], G. Kleppel[1], A. Steele[1], R. Iturriaga[1], and I. Haydock[2]

[1]University of Southern California
Los Angeles, CA 90089-0371

[2]Ocean Monitoring Section
Los Angeles County Sanitation District
Whittier, CA

ABSTRACT

The dispersion of a buoyant effluent plume has rarely been studied at intermediate to far field scales O(100 m-10 km) in the ocean. A comprehensive, interdisciplinary study of the interaction of an outfall plume with the coastal ocean was conducted during winter, 1985, off the coast of Los Angeles . During these observations, the plume modified the local stratification and the effluent was advected by the ambient flow field. The present study demonstrates that chemical, biological, and optical variables associated with an outfall plume may be effectively used to study the dispersion of buoyant plumes in the coastal ocean.

INTRODUCTION

The present study focuses upon the intermediate and far field variability of an ocean outfall plume and the natural processes that are primarily responsible for plume structure and evolution. Several processes generally affect the distribution of physical, chemical and biological variables in the ocean over a broad range of space and time scales. The specific problem of sewage effluent plume dispersion spans horizontal scales up to O(10 km) and time scales up to a few days.

The design of outfall diffusers and the initial dilution phase of the effluent, O(100 m), have been well documented by Fischer, et al. (1979). They have also reviewed theoretical and laboratory studies of buoyant plumes. Such plumes have also been relatively well studied in the atmosphere (e.g., Csanady, 1980). However, there have been few observational studies of buoyant plumes in the ocean at scales greater than those relevant to the initial dilution phase of the effluent.

Outfalls discharge traceable substances that enable the mapping of plumes in the natural environment. The distribution of an effluent field thus may be used for evaluating the advective and mixing

processes (as influenced by stratification) occurring in the vicinity of an ocean outfall. In addition, spatial and temporal changes in the effluent field distribution provide a means of quantifying responses to local physical forcing.

This study was primarily motivated by the need for observations of physical, chemical, and biological variable fields at space and time scales greater than those relevant to the initial dilution phase of the effluent discharge. The observations presented here were obtained during winter conditions (relatively weak seasonal stratification) off the Palos Verdes Peninsula, California (33°N, 118°W) near the site of the Los Angeles County Sanitation District's outfall diffusers (described in Fischer, et al., 1979). An account of some of our earlier work in this region may be found in Siegel, et al. (1986). Work concerning nutrients and phytoplankton in this region can be found in MacIsaac, et al (1979).

METHODS

The observational plan for this program was to employ several complementary sampling methods to determine the structure and distributions of tracer variable fields associated with an effluent plume along with the processes affecting the plume. The sampling included meteorological observations, satellite sea surface temperature mapping, Eulerian and Lagrangian current measurements, and 3-dimensional mapping of physical, chemical, biological, and optical variables. The observations made during January-May 1985 are summarized in Fig. 1. To emphasize the complementary nature of our observations, we focus on a subset of the data taken during January 1985.

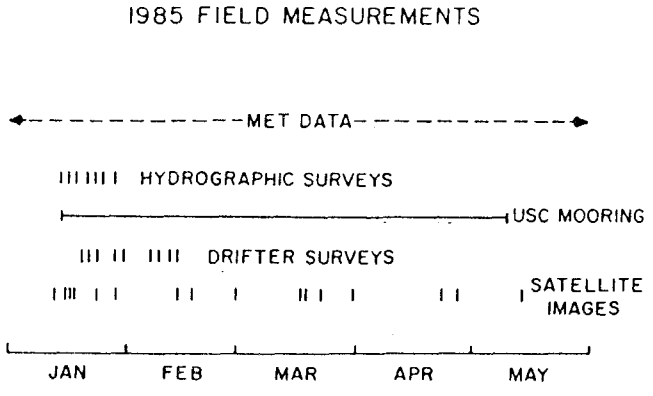

Figure 1. Time line of observations discussed for the 1985 field study of the region surrounding the Los Angeles County White's Point Outfall. For hydrographic and drifter surveys the vertical bars indicate sampling days. For the satellite images, the vertical bars indicate days when relatively clear images of the study area were obtained.

Spatial variability of the region was sampled using several methods. Larger scale sea surface temperature (SST) patterns were mapped using satellite infrared images (AVHRR sensors on NOAA-7 and -9 satellites). The archived images have been processed in order to resolve thermal features [O(10-100 km)] in the region from Santa Monica Bay to Long Beach Harbor and seaward about 70 kms (Fig. 2).

Figure 2. A satellite AVHRR image of sea surface temperature from January 23, 1985. The cooler temperatures are represented by the lighter shades of gray and the darker areas represent the warmer temperatures.

Smaller spatial scales were sampled with shipborne instrumentation. Three-dimensional hydrographic maps were obtained for the following variables: temperature, salinity, plant nutrients (nitrate - NO_3, nitrite - NO_2, ammonium - NH_4, silicate - SiO_4, and phosphate - PO_4), beam attenuation, chlorophyll fluorescence, phytoplankton pigments, and bacterial abundance and productivity (Jones, et al., 1983; Fuhrman and Azam, 1982; Standard Methods, 1981). Observations spanned the period from January 14 to 28, with mapping repeated approximately every 2 days. The sampling grid included a dense core grid around the outfalls with a station spacing of 1 km and an expanded grid with 2 km intervals both upcoast and downcoast from the core grid (as shown in Fig. 5). Continuous vertical

profiles of temperature, beam attenuation and fluorescence were obtained at all of the grid points and averaged using ~5 m vertical bins. Vertical pump profiles (~10 m resolution) of temperature, salinity, nutrients, chlorophyll, and bacterial abundance and productivity were obtained at 2 km intervals and sampling of the entire grid took approximately 10 hours.

Time series observations included meteorological variables (wind speed and direction) and moored measurements of horizontal currents and temperature. Meteorological data were obtained from a coastal station ~7 km upcoast from the study site and several other local meteorological stations. The current meter mooring had four instruments suspended at 14, 25, 36 and 47 m beneath the ocean surface. Two horizontal current components and temperature were measured with each instrument. The instruments employed were vector measuring current meters with thermistors (Weller and Davis, 1980). The mooring was located approximately 2 kms upcoast from the Los Angeles County outfalls and on approximately the same isobath as the outfall diffusers (~55 m total water depth, Fig. 5a). Details concerning the time series measurements may be found in Steele (1986).

In addition to moored current measurements, near-surface currents were measured on selected days in January and February with surface drifters that were tracked with the aid of a precision microwave ranging system. Arrays of 18-20 drifters were deployed in a cross-shaped pattern centered on the current meter mooring. The drifters were then repeatedly located (~5-8 times per deployment) using the range finding system and a small coastal vessel. The nominal location accuracy was O(10 m).

RESULTS

Outfall Effluent Characteristics

The Los Angeles County Sanitation District submerged ocean outfall system consists of 2 multiport diffusers (often modeled as line sources; Roberts, 1979; Fischer, et al, 1979) located on about the 55 m isobath and 2 km offshore of White's Point (Fig. 5a). During January, 1985, an average of 362 million gallons of effluent were released per day (1.37×10^{-3} $km^3 d^{-1}$) through the White's Point outfall. The initial dilution is considered to be about 100:1 (Fischer, et al, 1979) and may range from 80:1 to 300:1 (Mearns, 1981). The Froude number (as defined by Roberts, 1979) for the effluent during this period is O(0.5) assuming an average current velocity of 10 cm s^{-1}. Typical values for some of the constituents of the effluent including forms of inorganic nitrogen and total phosphorus are listed in Table 1. Also shown are the expected changes from ambient conditions when effluent water is mixed with the ambient seawater assuming 100:1 dilution. Ammonium nitrogen and total phosphorus yield the largest relative changes.

Satellite Mapping

The intensity of the cross-shelf SST gradient in the Southern California Bight varies seasonally and tends to be relatively weak during winter. An example of the winter structure is shown in an AVHRR satellite image from a clear day, January 23, during the hydrographic sampling period (Fig. 2). A band of cool water is coherent alongshore (southeast) for a distance of approximately 50 km. In the cross-shelf direction, the surface temperature is nearly isothermal from the coast to about 2.5 km offshore. Farther offshore the temperature gradually increases by about 0.4°C over 26 km. The range of SST over the entire image is about 2°C.

TABLE 1

Several characteristic values for effluent constituents from the Los Angeles County Sanitation District's White Point Outfall during January, 1985.

VARIABLE	EFFLUENT VALUE	EXPECTED AFFECT ON SEAWATER AFTER 100:1 DILUTION
Temperature(1)	26.4°C	+0.11°C (3)
NO_3-nitrogen(2)	5 μM	+0.05 μM
NO_2-nitrogen(2)	<0.7 μM	<0.007 μM
NH_4-nitrogen(2)	2.76 mM	+27.6 μM
Total phosphorus(2)	0.25 mM	+2.5 μM

(1) Average for January 1985
(2) 24 hour composite sample for January 9, 1985
(3) Assuming an ambient ocean temperature of 15°C

Time Series Observations

Time series of several pertinent physical quantities (Fig. 3a-e) were sampled over the same time period as the water column surveys. Specific days of interest are noted on the time axis. The planview map (Fig. 5a) shows the locations of the current meter mooring and a meteorological station which was positioned on a promontory (Point Vicente) ~6 km northwest of the mooring.

The alongshelf wind component (positive for a flow directed towards ~330° magnetic for both wind and currents) varies between ±6 m s^{-1} during most of the time interval. A local minimum (~11 m s^{-1}) occurs near midnight January 26, 1985. The cross-shelf wind component (positive onshore for both wind and currents) is less energetic and does not exceed 4 m s^{-1} in amplitude during this eleven day period. Diurnal sea breeze effects are not evident in the wind time series for this location and time domain.

Alongshelf current variability at 14 and 36 m depth levels (Fig. 3b) does not appear to be well correlated with local surface winds during this period. Currents vary mostly at near-tidal frequencies in response to barotropic and baroclinic tides. The maximum current amplitude observed during this period is ~20 cm s^{-1}. Compared to many other coastal environments with relatively narrow continental shelves, the currents at this location exhibit an anomalously low level of subtidal variability (Allen, et al., 1983). The largest values of alongshelf current shear (between the 14 and 36 m depth instruments) are O(5×10^{-3} s^{-1}) and occur during a period of elevated buoyancy frequency (January 26-29; Fig. 3e). The cross-shelf current components for the same depths and time interval (Fig. 3c) are generally smaller in amplitude (less than 10 cm s^{-1}), especially during the middle portion of the time series when density stratification is weak (January 23-26).

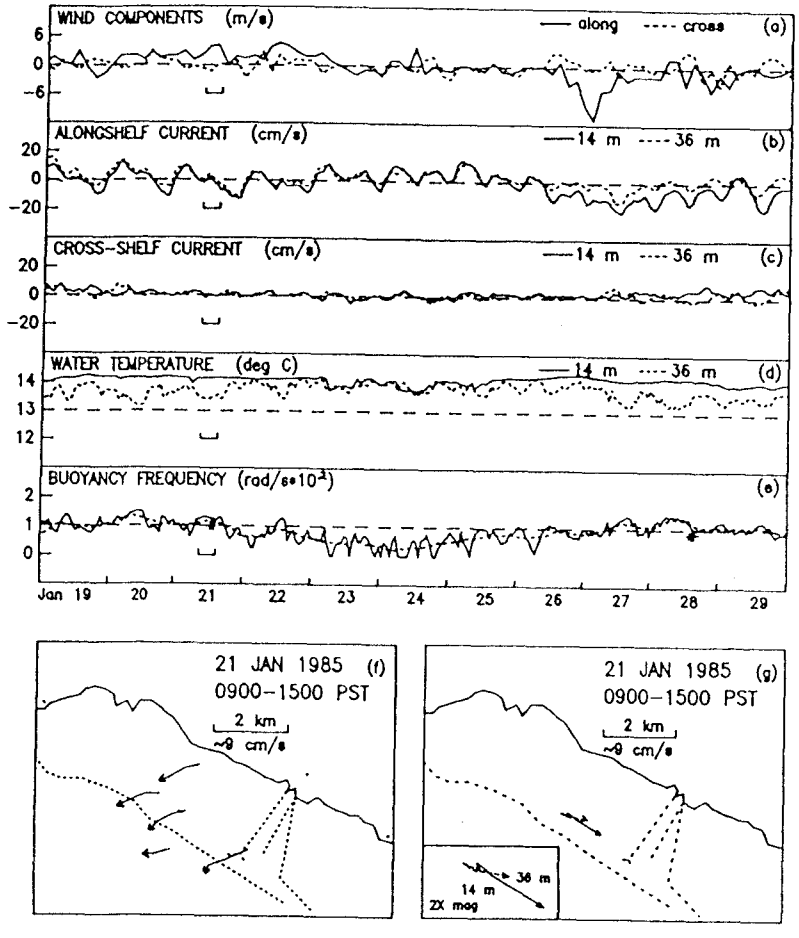

Figure 3. Time series of wind, currents and temperature for an eleven day period in January, 1985. The wind observations are from Point Vicente and the current meter observations from the mooring on the 55 m isobath (Fig. 5e). a) Time series of alongshelf and cross-shelf wind components. The alongshelf component is positive toward the northwest and the cross-shelf component is positive toward the northeast; b) Alongshelf current from the 14 and 36 m current meters; c) Cross-shelf current from the 14 and 36 m current meters; d) Temperature time series from the 14 and 36 m current meters; e) Time series of estimated buoyancy frequency (see text); f) Surface drifter trajectories for 0900-1500, January 21, 1985; g) Subsurface provessive vectors for 0900-1500, January 21, 1985.

Temperature time series are shown for 14 m and 36 m depth levels in Fig. 3d. The temperature fluctuations at 14 m are O(0.2°C) over the interval shown and the relative lack of variability is primarily due to the fact that this instrument is within the mixed layer a large percentage of the time. A higher degree of temperature variability is observed at 36 m with the overall range and largest short term fluctuations approaching 1°C. There is no obvious correspondence between temperature fluctuations at either of these two depths and wind or current fluctuations.

The time evolution of average buoyancy frequency (a difference estimate between 14 and 36 m depth levels, Fig. 3e) varies most noticeably over time scales of a few days with shorter term variability occurring primarily at semidiurnal time scales. Over this eleven day time interval, three distinct stratification regimes are observed. The first three days are marked by relatively intense stratification and moderate values of current shear. The following three days show weak stratification, minimal surface wind forcing, and almost no velocity shear between the 14 and 36 m depth levels. During the final four days, density stratification increases to a local maximum with elevated values of current shear in both horizontal current components.

Average buoyancy frequency values derived from mooring and hydrographic survey data (shown as asterisks in Fig. 3e) compare favorably (within ~10%) for the days when both types of data are available. An average T-S relationship derived from the hydrographic data was used to account for salinity induced density variability since salinity was not measured from the mooring. Salinity variations accounted for ~50% of the variance in the density field during this time period. Thus, individual density and density difference values have large error bounds, particularly when the water column is nearly isothermal. Rare temperature inversions are presumed to be salinity compensated in the density field.

The tracks of five surface drifters deployed over the interval 0900-1500, January 21, 1985 are shown in Fig. 3f. During this time period (highlighted with brackets in the time series plots), surface winds are directed upcoast and offshore at 2-4 m s^{-1}. Measured currents at 14 and 36 m depths increase from near 0 to 10 cm s^{-1} downcoast. The surface drifters move in a nearly uniform pattern upcoast and offshore at ~5 cm s^{-1}.

Integrated time histories of currents measured at 14 and 36 m depth levels are shown as progressive displacement vectors in Fig. 3g. These trajectories are downcoast and decrease with depth. Comparison of Figs. 3f and g suggests that there is significant velocity shear in the near-surface portion of the water column (the drifters are "tagged" to water parcels within 0.5 m of the free surface). This may indicate a short-term, localized response of the near-surface layer to wind forcing.

Spectra of the near-surface (14 m depth) current components and temperature fluctuations for the entire deployment period of mid-January through mid-May, 1985, are shown in Fig. 4. The spectra show significant energy concentrations at near-tidal frequencies with a smaller proportion of the variance in the current components for frequencies less than 1 cycle day^{-1}. This particular distribution of current variance contrasts with that of other coastal sites in the Southern California Bight (e.g. Winant and Bratkovich, 1981; Hendricks, 1980) which tend to have a greater percentage of variance (especially in the alongshelf component) associated with subtidal fluctuations.

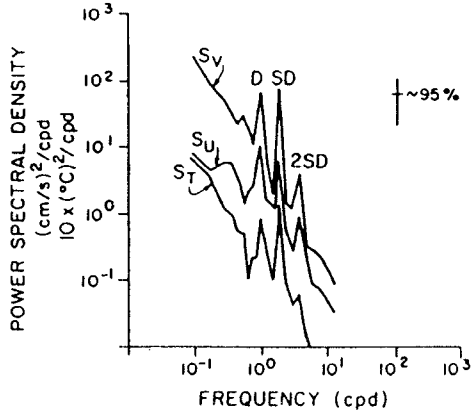

Figure 4. Power spectra (S_u-cross-shelf, S_v-alongshelf, S_t-temperature) of horizontal current components and temperature for the near-surface (14 m depth level) instrument. Overall duration of the time series used to form the spectra is ~107 days (January 15, 1985 through May 2, 1985). Spectral estimates are ensemble averages of individual values based upon a 10 day time interval. Diurnal, semidiurnal and twice semidiurnal peaks are marked with D, SD and 2SD, respectively.

Shipborne Mapping

The hydrographic mapping observations provide information on the distributions of the sampled variables in 3-dimensional space and on the average intervariable relationships. Results from January 21, 1985 are used to demonstrate the patterns observed.

The distributions of variables primarily indicative of the effluent field (e.g., ammonium, coliform bacteria, and bacterial cell productivity) show a near-surface manifestation on January 21, 1985 (Fig. 5). The distributions indicate that the effluent field is rising to the surface while slowly advecting downcoast, in the same direction indicated by the moored current meters. These three variables show similar surface patterns and appear to be effective tracers of the effluent field.

Three cross-shelf sections (Fig. 6) show the vertical structure associated with the surface field. The first section (X=0), located midway between the two outfall diffusers, shows a stratified temperature regime with a temperature decrease of 2.5°C from the surface to 80 m (Fig. 6a). The section of the square of the buoyancy frequency (N^2) shows maximum stratification at ~30 m near the coast deepening to about 40 m farther offshore and little stratification in the upper 20 m (Fig. 6b). A bolus of high ammonium (>5 μM) water occurs near the coast between 30 and 40 m depth (Fig. 6c). In the upper 20 m of the water

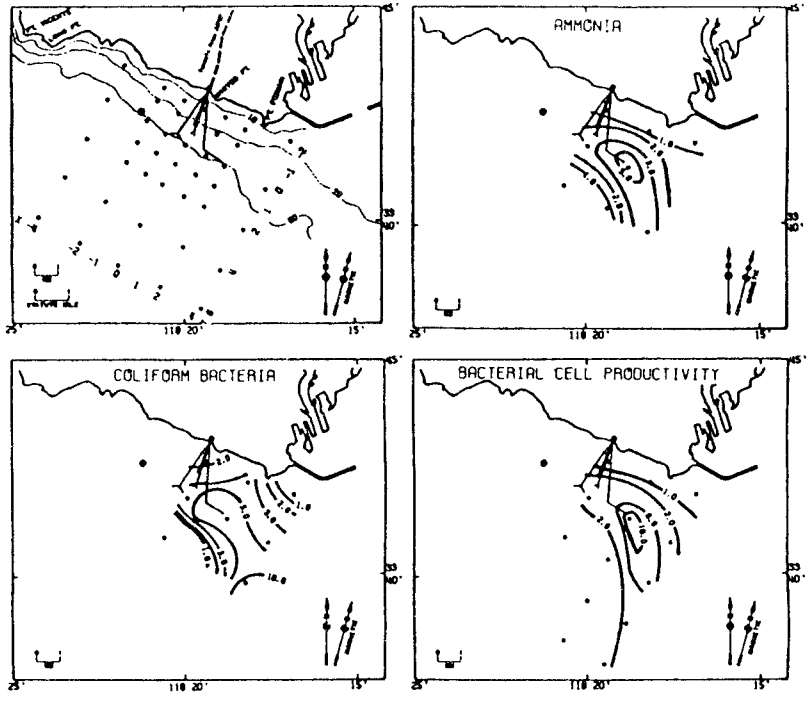

Figure 5. a) Locator map of hydrographic stations (dots), current meter mooring (circled dot), and meteorological station site (Pt. Vicente) for the region around the Los Angeles County White's Point Outfall. b) Surface ammonium concentrations (μM) for January 21, 1985. Dots indicate sampling locations. c) Surface coliform bacteria abundance (MPN) for January 21, 1985. d) Surface bacterial cell productivity (10^8 $l^{-1}d^{-1}$).

column, the isopleths (1 and 2 μM) open toward the surface, consistent with the weak stratification. Beam transmission (Fig. 6d) is lowest nearshore and increases both offshore and at depth. Chlorophyll fluorescence (Fig. 6e), which is not a component of the effluent, also is high nearshore and in the upper 20 m. The minimum chlorophyll fluorescence in the upper layer occurs in the middle of the transect where the ammonium, and hence the effluent influence, is greatest. Beam transmission and chlorophyll fluorescence tend to show similar trends. Increased chlorophyll fluorescence nearshore is correlated with decreased beam transmission in the upper layer. For each of the variables in this section, except N^2, the isopleths tend to have a vertical orientation in the upper 20 m where the weakest stratification is observed.

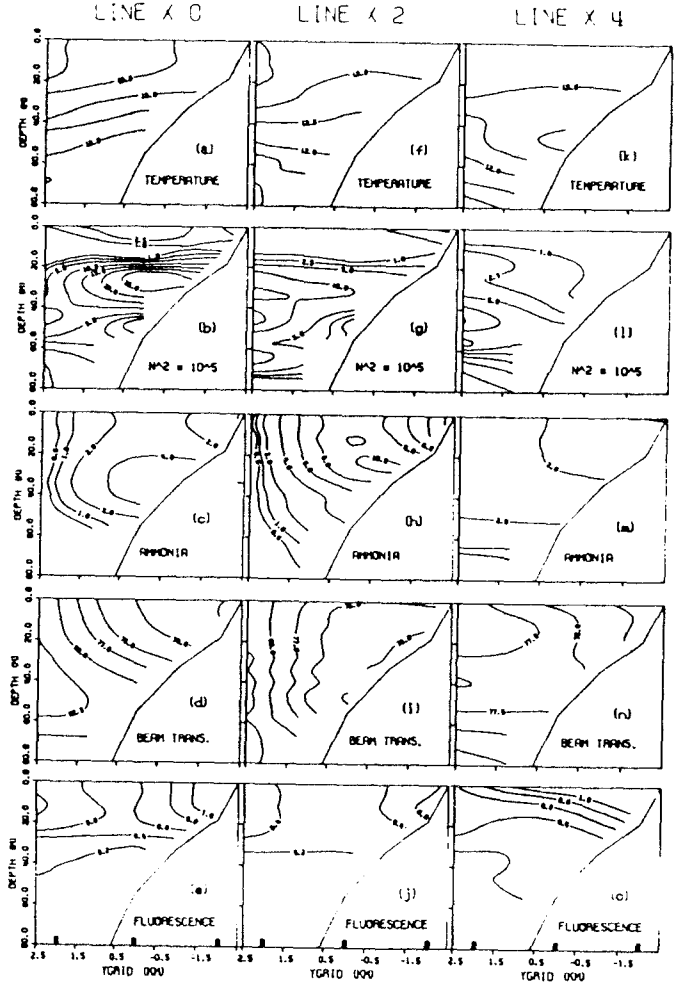

Figure 6. Cross-shelf hydrographic sections for January 21, 1985. The locations of the sections are indicated in Fig. 5a. Station locations are indicated by the vertical bars in the fluorescence plots (e, j, and o). Temperature units are °C; N^2 is in $(\text{rad s}^{-1})^2$; ammonium concentration is in μM; beam transmission units are percent transmission; and fluorescence units are relative.

The next section (X-2) is 2 km downcoast from the previous section and just beyond the end of the larger outfall diffuser (Fig. 6f-j). The temperature section (Fig. 6f) shows some differences from the previous section. The 13°C isotherm shallows to less than 20 m at midsection and temperatures greater than 13.5°C occur only at the offshore end of the section. The N^2 maximum (Fig. 6g) is about half that in the previous section, but occurs at about the same depth. Unlike the first section, the maximum N^2 decreases toward the coast. This decreasing trend in N^2 coincides with the region of high ammonium concentration near the bottom (Fig. 6h), suggesting the influence of the effluent. The maximum ammonium concentration is about twice that in the previous section. The upward bulge in the 13°C isotherm (Fig. 6f) coincides with the area of maximum ammonium concentration. This suggests that the effluent is entraining deeper, cool water as it rises toward the surface and thus weakens the stratification. Beam transmission (Fig. 6i) is lowest near the bottom in the vicinity of the ammonium maximum and increases offshore paralleling the decrease in ammonium concentration. This also indicates the effect of the plume. The chlorophyll fluorescence distribution (Fig. 6j) is similar to the pattern in the first section except that the area of the minimum in the center of the section is broader. This pattern is similar to that of ammonium concentration above 30 m and is indicative of the effluent. The effluent influence is greatest in this section. It appears to affect not only the concentration of effluent-derived constituents, but also seems to perturb the local stratification.

The final section (X-4) is an additional 2 km downcoast (Fig. 6k-o). Similar to the X-0 section, 13.5°C water is present in the upper 20 m across the entire section (Fig. 6k). The 12.5°C isotherm is somewhat deeper than in the previous section. Over the entire section stratification appears to be weaker and the maximum deeper (~40 m) than in either of the previous two sections (Fig. 6l). The ammonium concentrations (Fig. 6m) are not as great as in the other sections, but are still elevated, indicating the presence of effluent-derived water. The near-surface ammonium maximum is farther offshore suggesting some offshore advection. Beam attenuation (Fig. 6n) is again lowest near the coast increasing offshore and with depth. Chlorophyll fluorescence (Fig. 6o) is relatively high in the upper 20 m across the section and decreases only at the offshore end of the section. The 0.2 fluorescence isopleth is somewhat deeper at midsection, and follows the deepening of the 12.5°C isotherm.

These hydrographic sections may be interpreted in the following general way. The effluent rises toward the surface (line X-2, Y=-1.5). Currents are advecting the effluent (as it is being mixed with ambient water) primarily downcoast (toward line X-4). The influence of the effluent increases from the upcoast section (X-0, nearest the upcoast diffuser) downcoast to the X-2 section where the input of the second diffuser is also manifest. Farther downcoast from the two diffusers at the X-4 section the effluent signal has decreased. The diminishing concentrations of effluent-related variables downcoast may also be due to the divergence (and possible curvature) of the flow field. While the effluent field is most apparent in ammonium and beam transmission, there appears to be a significant effect upon the ambient stratification and fluorescence.

Although the winter is considered to be a period of weak stratification, a layer of relatively intense stratification in the water column is observed. This stratification is not great enough to limit the

effluent field to subthermocline depths, but it is sufficient to alter the patterns observed in the vertical distributions of the effluent field. Along the X-2 section, the stratification is apparently reduced by the presence of the effluent plume.

This data set indicates that there are two components of the overall hydrography in the region near the outfalls. The dominant component is that of the ambient ocean and is most clearly reflected in temperature, nitrate, silicate, and chlorophyll. The second component contributing to variability in the hydrographic fields is the effluent component. The effluent component is particularly evident in the following variables: ammonium, phosphate, coliform bacteria abundance, bacterial productivity, and beam transmission. The intervariable relationships are clearly resolved using a multivariate statistical aproach, principal component analysis (Legendre and Legendre, 1983). The results from the analysis of the data from 21 January are shown in Table 2 . The first principal component accounts for 38% of the total variance in the data set and represents the variance due to the ambient ocean. The relative contributions of variables to this component are indicated in the loadings of the variables, which essentially represent correlations of the given variable with the component. Temperature, nitrate, silicate, and chlorophyll most strongly correlate with this component. The second principal component represents the effluent field as indicated by the high loadings for ammonium, salinity, and phosphate. This component accounts for 26% of the variance. Although not included in the statistical analysis, coliform bacteria abundance and bacterial productivity are well correlated with this component of variance.

TABLE 2

The loadings of the variables from the pump profiling performed on January 21, 1985, for the first two principal components resulting from the analysis. The numbers in parentheses indicate the percentage of the variance accounted for by each component. The analysis included 42 observations.

Principal Component Loadings

	1 (38%)	2 (26%)
Temperature	-0.92	-0.11
Salinity	0.52	-0.76
Sigma-t	0.85	-0.47
NO_3	0.86	0.03
NO_2	0.33	0.24
NH_4	0.04	0.87
SiO_4	0.86	0.38
PO_4	0.43	0.75
Chlorophyll a	0.05	-0.53
Phaeopigment	-0.44	0.15

SUMMARY

An outfall plume in the coastal environment was comprehensively mapped and some of the processes that affect plume evolution were determined. Several complementary sampling methods enabled the resolution of a broad range of space and time scales relevant to an oceanic, buoyant plume during winter-time, weakly stratified conditions.

Wind and current fluctuations were observed to have relatively small amplitudes during this period. Alongshelf current variability was dominated by near-tidal rather than subinertial components in contrast to other coastal sites in the Southern California Bight. These conditions may have contributed to stronger density stratification and higher near-surface water temperatures than normally observed.

The hydrography during this period was dominated by two components: the ambient ocean and the outfall effluent field. The perturbation of the ambient hydrographic conditions was much larger for ammonium, phosphate, and bacterial parameters than for temperature and salinity. Other factors which affect the biochemical variables (e.g., biological growth and death, and nutrient uptake) must ultimately be considered. The general distribution of the effluent field was skewed downcoast in the direction of the prevailing currents. In the vicinity of outfall, the stratification appeared to be weakened by the effluent field. Significant spatial variability was associated with the interaction between the effluent and the ambient field. With weak advection (<10 cm s^{-1}) and moderate stratification, the effluent field was confined to a relatively small spatial region.

Three relatively distinct stratification regimes occurred during the course of this study interval. The first (detailed in the present work) was a three day period of greater density stratification and weak current shear. The second regime was a period of weak wind forcing, weak density stratification, and minimal current shear. During the third period, density stratification reintensified and current shear was enhanced in both horizontal current components.

To our knowledge, this is one of the most comprehensive and integrated process-oriented field studies of an oceanic buoyant plume. It has been shown that chemical, biological, and optical variables associated with an outfall effluent may be effectively used to study the dispersion of buoyant plumes in the coastal ocean. These types of data may also be used to supplement and interpret physical observations. Analysis of this data set is continuing and we expect that the results may be useful for modeling the dispersion of buoyant plumes in the coastal environment.

ACKNOWLEDGEMENTS

This work has been supported by the University of Southern California Sea Grant Program and by the Los Angeles County Sanitation District. We thank David Siegel for stimulating discussions and assistance at sea, and Eric Olson, Pat Cascallar and Rustin Erdman for technical assistance.

REFERENCES

Allen, J. S., R. C. Beardsley, J.O. Blanton, W. C. Boicourt, B. Butman, L. K. Coachman, A. Huyer, T. H. Kinder, T. C. Royer, J. D. Schumacher, R. L. Smith, W. Sturges, and C. D. Winant, Physical oceanography of continental shelves, Reviews of Geophysics and Space Physics, 21, 1149-1181, 1983.

Csanady, G. T., Turbulent Diffusion in the Environment, Reidel, 248 p., 1980.

Fischer, H. B., E. J. List, R. C. Y. Koh, J. Imberger, and N. H. Brooks, Mixing in Inland and Coastal Waters, Academic Press, New York, 1979.

Fuhrman, J. A. and F. Azam, Thymidine incorporation as a measure of heterotrophic bacterioplankton production in marine surface waters, evaluation and field results, Mar. Biol., 66, 109-120, 1982.

Hendricks, T. J., Currents in the Los Angeles Area, in Southern California Coastal Water Research Project, Biennial Report, 1979-1980, edited by W. Bascom, 243-257, 1980.

Jones, B. H., K. H. Brink, R. C. Dugdale, D. W. Stuart, J. C. VanLeer, D. Blasco, and J. C. Kelley, Observations of a persistent upwelling center off Point Conception, California, in Coastal Upwelling, edited by E. Suess and J. Thiede, Plenum, New York, 1983.

MacIsaac, J., R. C. Dugdale, S. A. Huntsman, and H. L. Conway, The effect of sewage on uptake of inorganic nitrogen and carbon by natural populations of marine phytoplankton, J. Mar. Res., 37, 51-66, 1979.

Mearns, A. J., Ecological effects of ocean sewage outfalls: observations and lessons, Oceanus, 24, 45-54, 1981.

Siegel, D., B. Jones, T. Dickey, I. Haydock, and A. Bratkovich, Physical and biological variability near the White's Point, California ocean outfall, in Proceedings of the Fifth International Ocean Disposal Symposium, edited by I. Duedahl, 1986.

Standard Methods for the Examination of Water and Waste, 15th ed., American Public Health Association, Washington, D.C., 1981.

Steele, J. A., Variability in Temperature in Coastal Waters near the Palos Verdes Peninsula between January and May 1985, Masters Thesis, University of Southern California, Los Angeles, 104 pp., 1986.

Weller, R. A., and R. Davis, A vector measuring current meter, Deep-Sea Research, 27, 565-582, 1980.

Winant, C. D. and A. W. Bratkovich, Temperature and Currents on the southern California shelf: A description of the variability, J. Phys. Ocean., 11, 71-86, 1981.